Science of the Total Environment 470–471 (2014) 488–500

Contents lists available at ScienceDirect

Science of the Total Environment

journal homepage: www.elsevier.com/locate/scitotenv

# Effects of river morphology, hydraulic gradients, and sediment deposition on water exchange and oxygen dynamics in salmonid redds

Y. Schindler Wildhaber [a,*,1], C. Michel [b,1], J. Epting [c], R.A. Wildhaber [a], E. Huber [c], P. Huggenberger [c], P. Burkhardt-Holm [b,d], C. Alewell [a]

[a] Institute for Environmental Geosciences, Bernoullistr. 30, 4056 Basel, Switzerland
[b] Man–Society–Environment MGU, Vesalgasse 1, 4051 Basel, Switzerland
[c] Applied and Environmental Geology, Bernoullistr. 32, 4056 Basel, Switzerland
[d] Department of Biological Sciences, University of Alberta, Edmonton, Canada

## HIGHLIGHTS

- Hyporheic exchange and oxygen are crucial for survival in redd and highly variable.
- Oxygen and water exchange are affected by fine sediment, $C_{org}$ and redd morphology.
- Artificial steps in canalized river are positive in high flow section, and negative in low flow section.
- Measurement of crucial parameters in artificial redd was successful.
- Considerable work investment is needed for these measurements.

## ARTICLE INFO

*Article history:*
Received 12 May 2013
Received in revised form 27 September 2013
Accepted 29 September 2013
Available online 26 October 2013

Editor: Christian EW Steinberg

*Keywords:*
Sediment infiltration
Sediment accumulation
Specific infiltration rate
Swiss Plateau
River modification
Brown trout

## ABSTRACT

Fine sediment decreasing gravel permeability and oxygen supply to incubating salmonid embryos, is often considered the main contributing factor for the observed decline of salmonid populations. However, oxygen supply to salmonid embryos also depends on hydraulic conditions driving water flow through the redd. A more generalized perspective is needed to better understand the constraints on successful salmonid incubation in the many heavily modified fluvial ecosystems of the Northern Hemisphere. The effects of hydraulic gradients, riverbed and redd morphology as well as fine sediment deposition on dissolved oxygen (DO) and water exchange was studied in 18 artificial redds at three sites along a modified river. Fifty percent of the redds in the two downstream sites were lost during high flow events, while redd loss at the upstream site was substantially lower (8%). This pattern was likely related to increasing flood heights from up- to downstream. Specific water infiltration rates (q) and DO were highly dynamic and driven on multiple temporal and spatial scales. Temporally, the high permeability of the redd gravel and the typical pit–tail structure of the new built redds, leading to high DO, disappeared within a month, when fine sediment had infiltrated and the redd structure was leveled. On the scale of hours to days, DO concentrations and q increased during high flows, but decreased during the falling limb of the water level, most likely related to exfiltration of oxygen depleted groundwater or hyporheic water. DO concentrations also decreased under prolonged base flow conditions, when increased infiltration of silt and clay particles clogged the riverbed and reduced q. Spatially, artificial log steps affected fine sediment infiltration, q and interstitial DO in the redds. The results demonstrate that multiple factors have to be considered for successful river management in salmonid streams, including riverbed structure and local and regional hydrogeological conditions.



## 1. Introduction

Native salmonid populations are declining in numerous countries around the world, including populations of brown trout *Salmo trutta* in Switzerland (Burkhardt-Holm and Scheurer, 2007), Atlantic salmon *Salmo salar* in the United Kingdom (Youngson et al., 2002) and coho salmon *Oncorhynchus kisutch* in North America (Brown et al., 1994). Habitat degradation is considered a major threat for native salmonids (e.g., Brown et al., 1994; Burkhardt-Holm and Scheurer, 2007; Gilvear et al., 2002; Hicks et al., 1991). In this regard, fine sediment (<2 mm) deposition has been argued as the single contributing factor (e.g., Jensen et al., 2009 and studies cited therein). Deposited fine sediment

* Corresponding author.
*E-mail address:* yael.schindler@eawag.ch (Y. Schindler Wildhaber).
[1] Shared first authorship.

0048-9697/$ – see front matter © 2013 Elsevier B.V. All rights reserved.
http://dx.doi.org/10.1016/j.scitotenv.2013.09.100

can decrease redd gravel permeability and interstitial flow (e.g., Brunke, 1999; Schälchli, 1995), which, in turn, hinders oxygen supply to incubating salmonid embryos, thereby affecting their survival (S. Greig et al., 2007; Greig et al., 2005; Heywood and Walling, 2007). However, the oxygen supply to incubating salmonids embryos depends on several further factors such as the relative contribution of oxygenated river water infiltration and exfiltration of oxygen depleted groundwater or interstitial water in the redd (Malcolm et al., 2006, 2009) or the oxygen demand of organic material (S.M. Greig et al., 2007). Although these factors vary extensively both temporally and spatially (Brunke and Gonser, 1997; S.M. Greig et al., 2007; Malcolm et al., 2006), only a few studies have resolved these processes on appropriate temporal and spatial scales.

Modeling approaches on the redd scale indicate that hyporheic velocities and dissolved oxygen (DO) concentrations within the egg pocket are enhanced due to the spawning activity, leading to reduced fine sediment and thus higher hydraulic conductivity (Tonina and Buffington, 2009; Zimmermann and Lapointe, 2005). Redd scale hyporheic exchange, measured on a centimeter to meter scale, can also be induced by the pit–tail structure of salmonid redds (Fig. 1A, Tonina and Buffington, 2009). This initial structure cannot, however, be expected to remain intact during high flow events (Ottaway et al., 1981). Hence hydraulic conditions on the redd scale likely change during the incubation season. Moreover, recent research clearly indicates the need for a multi-scale approach when investigating the dynamics of abiotic conditions in salmonid redds (Baxter and Hauer, 2000; Zimmermann and Lapointe, 2005): the local scale covers a single redd with an applied data grid resolution down to single centimeters (Fig. 1A). The intermediate scale covers the wider redd surrounding area of the riverbed including the relevant neighboring riverbed steps (Fig. 1B). The chosen data grid for this intermediate scale is in the range of meters. The regional scale considers a larger section of the river with a length and width of tenths of meters up to several kilometers (Fig. 1C). Hydraulic processes driven at all these scales can be expected to affect water exchange in a particular redd, and hence oxygen supply to the incubating embryos (Baxter and Hauer, 2000; Malcolm et al., 2008).

In Western Europe and North America many rivers with viable salmonid populations are heavily modified, i.e., channelized and with lateral stabilizations and artificial steps introduced for slope reduction (Brookes, 1988; Gilvear et al., 2002; Wohl, 2006). In channelized rivers, the lack of geomorphic features can substantially reduce hyporheic exchange (Malcolm et al., 2010), whereas hydraulic gradients related to artificial steps can markedly increase hyporheic exchange (Endreny et al., 2011). Artificial steps generate predictable flow-paths, with increased river water downwelling above steps and upwelling of hyporheic water below steps (Fig. 1B, e.g., Gooseff et al., 2006; Huber et al., 2013; Kasahara and Hill, 2006). Accordingly, artificial steps can increase hyporheic exchange in modified rivers (Kasahara and Hill, 2006; Sawyer et al., 2011) and could thereby also affect water exchange and oxygen supply in salmonid redds. Despite this, the effects of artificial steps on abiotic conditions in salmonid redds have, to our knowledge, not been investigated. This knowledge would provide important input for process-based river management in the many heavily modified salmonid streams of the Northern Hemisphere (e.g., Gilvear et al., 2002; Newson et al., 2012).

To this end, the current study evaluates the relative contribution of fine sediment, hydraulic gradients, river morphology, and regional geomorphology to specific water infiltration and oxygen dynamics in artificial brown trout redds in the Enziwigger, a heavily modified headwater river of the Swiss Plateau in the Canton of Lucerne. The Enziwigger also maintains a viable brown trout population (Schager et al., 2007).

The objective of this study was to provide a detailed investigation of the factors affecting the abiotic redd environment in a heavily modified river including I) an investigation of fine sediment deposition, hydraulic conditions (i.e., specific infiltration q, vertical and horizontal hydraulic gradients, and water level) and their effects on oxygen dynamics in the redds, II) an assessment of the morphological change of the riverbed and of the characteristic pit and tail structure of the redds and III) a comparison of the measured data with the results of a groundwater flow model, which was set up for one of the three experimental sites (cf. Huber et al., 2013). This model predicts zones of increased downwelling river water above steps, of hyporheic water upwelling

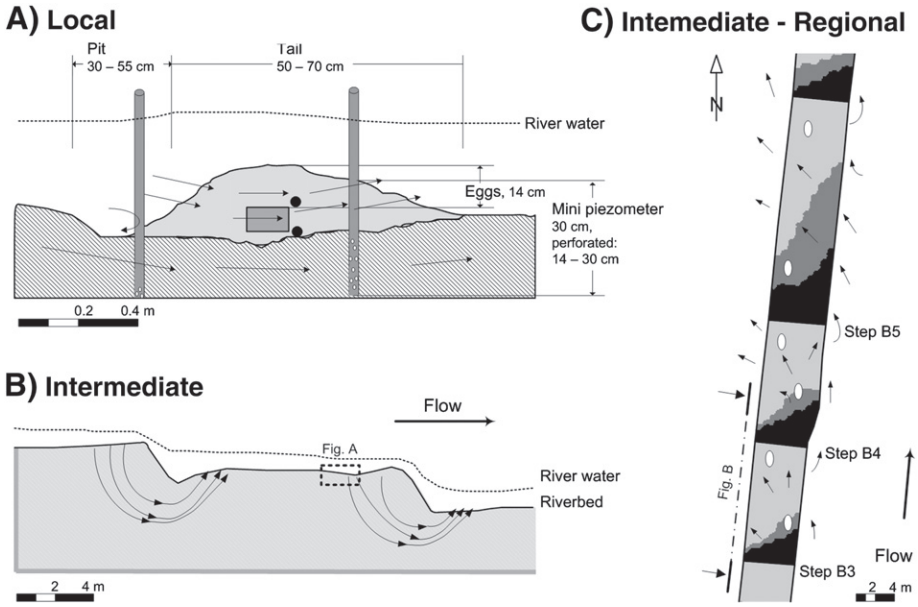


**Fig. 1.** Schematic view of (A) longitudinal section of an artificial redd (modified after Greig et al., 2007b) including the location of the mini-piezometers, the egg pockets (square) and temperature probes (bullet points) with the local scale flow pattern, (B) the hyporheic flow on an intermediate scale induced by riverbed steps according to the model calculations of Huber et al. (2013), and (C) the intermediate and regional scale water exchange processes (top view). Modeled river–groundwater exchange zones from Huber et al. (2013). Black: only exfiltration, gray: exfiltration and infiltration, light gray: only infiltration. Arrows indicate the main direction of the interstitial and groundwater flow, ovals represent the positions of the redds (for naming see Fig. 2).

below steps and zones with altering upwelling, downwelling and horizontal advection zones between the two steps.

In contrast to most previously published studies, data were collected with high spatial and temporal resolution (i.e., weekly or continuously) to explicitly characterize the temporal and spatial dynamics of the measured parameters. Measured parameters affect brown trout embryo survival in the redds and our results can thus be integrated with studies monitoring survival success of salmonid embryos (Michel et al., in revision), providing a more complete perspective on the factors affecting salmonid incubation success in comparable anthropogenically modified river environments.

## 2. Materials and methods

### 2.1. Study site and general setup

The river Enziwigger is a small channelized river located near Willisau, Canton of Lucerne, Switzerland with a total watershed area of about 31 $km^2$ (Fig. 2). Mean discharge, measured in Willisau (Fig. 2) by the Cantonal authorities (Nov. 2007–Nov. 2008) was 2.1 $m^3 s^{-1}$, minimum and maximum discharge were 1.1 $m^3 s^{-1}$ and 10.1 $m^3 s^{-1}$, respectively. During the 20th century the Enziwigger was straightened and channelized, and cross-channel log steps were installed as slope breakers to prevent deep channel erosion and bed-scouring during flood events (Fig. 2). Thus, like for most rivers in the Swiss Plateau, its morphology is strongly modified: only 5% is close to natural or natural, 21% is slightly affected and 74% is strongly affected or even artificial (classified with the Swiss modular stepwise procedure for ecomorphology after Huette and Niederhauser, 1998; Stucki, 2010). Despite these extensive modifications, its biological condition, classified with the macrozoobenthos module of the Swiss modular stepwise procedure (Stucki, 2010), is considered good (EBP-WSB-Agrofutura, 2005). The only fish species in the Enziwigger is the brown trout *S. trutta*, which maintains a viable population (EBP-WSB-Agrofutura, 2005; Schager et al., 2007). The flow regime of the Enziwigger is affected neither by hydro-power facilities nor by effluents from waste water treatment plants.

Measurements were conducted at three experimental sites along the river named A, B and C (from upstream to downstream; Fig. 2) at altitudes from 757 to 583 m a.s.l. The groundwater flow model was set up for site B (Huber et al., 2013). The riverbed at all sites is stabilized with artificial log steps, which strongly affect hyporheic exchange on an intermediate scale with river water infiltration upstream of the steps and exfiltration of hyporheic water downstream of the steps (Fig. 1B). At site A, the bedrock beneath the riverbed lies at a depth of a few decimeters and the hydrogeologic settings are assumed to be dominated by lateral inflow or the exfiltration of groundwater and/or hyporheic water. Piezometer measurements at sites B and C and the groundwater flow modeling at site B indicate on a regional scale a hydraulic gradient from the river to the main valley aquifer on the left side of the river and consequently a domination of river water infiltration (Fig. 1C, Huber et al., 2013). The influence of river flow stage and transient hillside groundwater flow has a minor impact on these intermediate and regional flow patterns (Huber et al., 2013).

Each site was equipped with six artificial salmonid redds in places wherein natural brown trout redds had been mapped in November 2008. The artificial redds were built to create a structure that resembles the structure of natural brown trout redds (Crisp and Carling, 1989). A detailed description of the redd structure and how it was built is given in Michel et al. (in revision). In the Enziwigger, these locations are mostly consistent from year to year (P. Amrein, Fish and Wildlife Service, Canton of Lucerne, pers. comm.). Data were collected during two spawning seasons (season 1 (S1): November 2009 to end of March 2010; season 2 (S2): November 2010 to end of March 2011) in 18 artificial redds per year (n = 36 redds in total). Redds were built in the same location each season (Fig. 2) with the exception of redds A31 and A32, which were covered in ice in January and February, making sampling impossible. Redds are labeled after the site (A, B, C), the terraces between two steps (1–5), the redd location within a terrace (1 and 2) and the season (S1 and S2). For example, redd A41_S1 identifies the first redd in the fourth investigated terrace at site A during

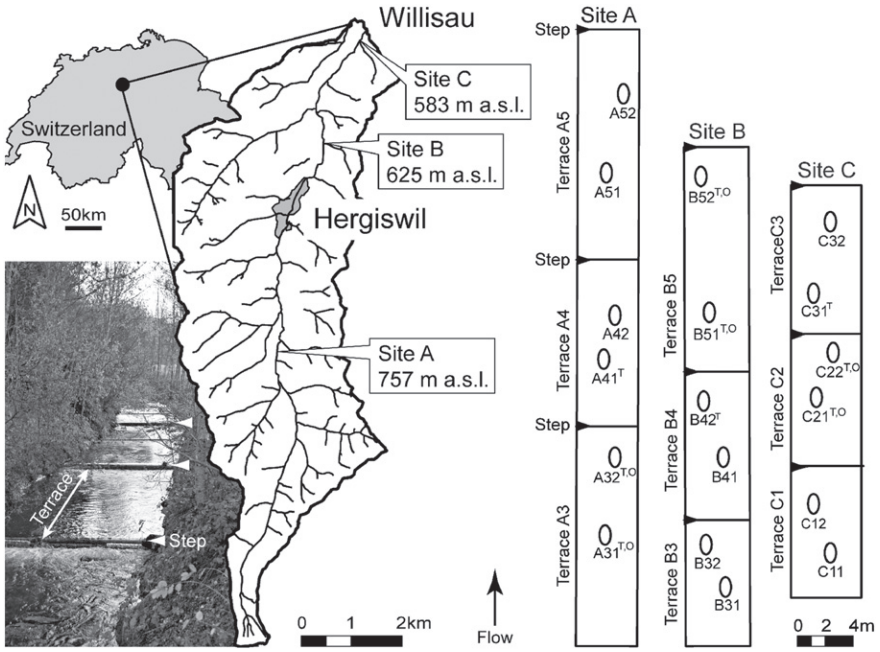


**Fig. 2.** Location of the Enziwigger watershed in Switzerland. The photograph shows the step and terrace structure at study site B. The watershed map of the river Enziwigger and the towns Willisau and Hergiswil (Canton of Lucerne, Switzerland) shows the locations of the three field sites A, B and C, while the schematic on the right illustrates the location of the redds within each field site. Here, superscripts indicate redds with continuous temperature (T) and oxygen (O) measurements.

the first season (Fig. 2). A detailed description of the river characteristics and field locations is given in Schindler Wildhaber et al. (2012b).

### 2.2. Sediment collection and analyses

Each redd was equipped with two sediment baskets to assess weekly fine sediment infiltration and net fine sediment accumulation during the entire field season (cf. Acornley and Sear, 1999; Greig et al., 2005; Heywood and Walling, 2007). One of them was emptied at weekly intervals to measure the weekly infiltration rates (= infiltration basket). The second set of sediment baskets was emptied at the end of the incubation season to measure net accumulation of fine sediment during the incubation period (= accumulation basket, Sear et al., 2008). At each site, the sediment basket data were complemented with four to seven freeze core samples to characterize the sediment stratification of the undisturbed river gravel. For a detailed description of the used baskets, the freeze core technique and their handling see Schindler Wildhaber et al. (2012b).

Grain size distribution was measured in a subsample of the fine sediment fraction of the freeze cores' layers 0–10 cm, 10–20 cm and 20–30 cm and in two subsamples of the fine sediment collected in accumulation baskets. Representative subsamples were obtained by a sample divider (Retsch, Haan, Germany). Additionally, grain size distributions of weekly infiltrated fine sediment samples ($n = 80$) were determined. The rest of the infiltrated fine sediment was pooled for each redd and a subsample was analyzed to obtain a mean grain size distribution of the infiltrated fine sediment. Grain size fractions were named according to the German soil taxonomy standard (DIN EN ISO 14688-1): sand: 0.063–2 mm, silt: 0.002–0.063 mm and clay: <0.002 mm (Sponagel et al., 2005).

Porosity (n) was calculated for each site on the basis of sediment grain size distributions from freeze core samples by the formula

$$n = 48.6 \cdot C_u^{-0.2}. \quad (1)$$

Where $C_u = d_{60}/d_{10}$ (diameter of grain size at the 60th and 10th percentile of the cumulative sample mass) (Schälchli, 1995).

The Fredle index of the accumulation baskets and of the freeze core samples was calculated by the formula

$$\text{Fredle index} = \frac{d_g}{S_o} \quad (2)$$

where $d_g$ is the geometric mean grain size and $S_o$ is the sorting coefficient derived by taking the square root of the quotient of the grain size at the 75th percentile divided by that at the 25th percentile (Lotspeich and Everest, 1981). The Fredle index is a central tendency quality index of the redd gravel composition, which gets smaller with smaller permeability of the sediment.

### 2.3. Oxygen

Continuous oxygen measurements were conducted with Aanderaa oxygen optodes 3835 (Aanderaa Data Instruments, Bergen, Norway) buried at the same depth as the incubating brown trout embryos (approx. 14 cm, cf. Michel et al., in revision). Oxygen contents in $mg\,l^{-1}$ as well as saturation (%) were measured every 10 s and mean values were logged in 10 min intervals. One optode per site was installed during season 1 (redds A32, B51 and C21) and two during season 2 (Fig. 2). Moreover, oxygen concentrations in each redd were measured manually every second week in mini-piezometers located in the pit and tail of each redd (Fig. 1A) with PreSens oxygen dipping probe minisensor (PreSens Precision Sensing GmbH, Regensburg, Germany). Each manual oxygen measurement was conducted twice: once in the "old" interstitial water and once in the refluent "new" water approximately 30 min after the "old water" had been extracted.

### 2.4. Riverbed and redd morphology

Riverbed morphology was mapped at a 0.5 m horizontal resolution in season 1 shortly after redd construction (October 26th 2009) and on December 27th after several high flow events. These data were used to assess morphological changes induced by high flow events on the river segment scale. The water depths above the deepest point of the pit and the highest point of the tail were measured weekly to quantify temporal changes of the typical redd structure.

### 2.5. Hydraulic investigations

Flow-stage at each site was measured every 15 s with pressure transmitter probes (STS, Sensor Technik Sirnach, Switzerland) and average values were logged at 10 min intervals during both field seasons.

Water levels above the pit and tail of each redd were recorded weekly to assess water level heterogeneity within sites. Vertical hydraulic gradients (VHGs) in the redds were measured weekly after Baxter et al. (2003) in mini-piezometers installed in the pit and tail of each redd (Fig. 1; for details see Schindler Wildhaber et al., 2012b). The VHG is a dimensionless parameter calculated by the formula

$$\text{VHG} = \frac{\Delta h}{\Delta l} \quad (3)$$

where $\Delta h$ is the difference in head between the water level in the piezometer and the level of the stream surface and $\Delta l$ is the depth from the streambed surface to the first holes in the piezometer (Baxter et al., 2003). Positive values indicate an energy gradient potentially sufficient to produce upwelling and negative values indicate an energy gradient potentially sufficient to produce downwelling. In the following, the VHG values are reported as upwelling or downwelling processes, although they are actually only a measure of upwelling and downwelling potential (Baxter and Hauer, 2000). The differences in VHGs between the pit and the tail piezometer of each redd were defined as the horizontal hydraulic gradients (HHGs), which is an indicator for hydraulic gradients driving water flow through the redd.

To obtain the temporal and spatial change of specific infiltration rates (q) in the redds, the one-dimensional heat pulse method was used (e.g., Hatch et al., 2006). For this, stream water temperature and temperatures at two different depths just above and below the incubating brown trout embryos (approx. 12 and 20 cm, respectively) were recorded every minute using thermocouple temperature probes (Campbell Scientific 105 E). Three redds per site were equipped with one or two temperature probes (Fig. 2). In redds equipped with two temperature probes, q could be calculated for the upper part ($q_u$, 0 to about 12 cm), the bottom part ($q_b$, about 12 cm to about 20 cm) and the total part ($q_t$, 0 to about 20 cm). In redds with one temperature probe, q could only be assessed in the upper part. The diurnal amplitude variations in temperature in the different depths and the diurnal phase variations were used to calculate q, but only the results of the former method were incorporated into further interpretations because of their higher stability. The method used allowed the calculation of two specific infiltration rate values per day.

The diurnal sinusoidal alternation was filtered from the temperature data by a discrete bandpass filter (FIR-filter with Hamming-window, 5001 filter coefficients, cut-off frequency $0.8 \cdot f_{Day}/1.5 \cdot f_{Day}$). All field temperature data were sampled with a frequency of one measurement per minute. When field sample periods exceeded 1 min, e.g., due to technical problems, linear interpolation was used to fill gaps of up to 10 min. Data gaps exceeding 10 min were marked as missing and not further evaluated. Data-points with time offset between the daily minima or maxima peaks of the corresponding sinusoidal temperature curves at the different depths exceeding 20% of a day period (i.e., 288 min) were also removed from further processing. The resulting temperature amplitude ratio ($A_r$) was used to estimate q.

The specific infiltration rate q and the vertical flow velocity ($v_f$) are extracted according to Eq. (4) (Ingebritsen et al., 2006) and Eq. (5) (Hatch et al., 2006, slightly transposed).

$$q = v_f \cdot n \tag{4}$$

$$v_f = \left(\frac{\rho \cdot c}{\rho_f \cdot c_f}\right) \cdot v. \tag{5}$$

For parameter definition and values see Table 1. The vertical fluid velocity (v) can be determined by the amplitude ratio ($A_r$), identified as $v_{Ar}$. The values were gained by a numerical solver from the Eqs. (6) and (7) (Hatch et al., 2006)

$$\frac{2\kappa_e}{\Delta z} \ln\left(A_r + \sqrt{\frac{\alpha(v_{Ar}) + {v_{Ar}}^2}{2}}\right) - v_{Ar} = 0 \tag{6}$$

where

$$\alpha(v) = \sqrt{v^4 + \left(8\pi \cdot f_{Day} \cdot \kappa_e\right)^2}. \tag{7}$$

The effective thermal diffusivity ($\kappa_e$) is estimated according to Hatch et al. (2006) by the equation

$$\kappa_e = \frac{\sigma}{\rho \cdot c} + \beta \cdot |v_f| \tag{8}$$

where the components of the first term are gained from:

$$\sigma = n \cdot \sigma_f + (1-n) \cdot \sigma_s \tag{9}$$

$$\rho = n \cdot \rho_f + (1-n) \cdot \rho_s \tag{10}$$

$$c = \frac{n\rho_f c_f + (1-n)\ \rho_s c_s}{n\rho_f + (1-n)\ \rho_s}. \tag{11}$$

The second term of the Eq. (8) was excluded from the calculations as its contribution to the value of $\kappa_e$ is negligible with the thermal dispersivity ($\beta$) $= 1 \cdot 10^{-3}$ as proposed by Hatch et al. (2006) and Keery et al. (2007) but it would strongly increase the complexity of the analysis (Keery et al., 2007).

Heat is mainly transferred through riverbed sediments by advection and conduction. Heat advection describes the heat transfer related to water flow through the sediment, while heat conduction describes the molecular transport of thermal energy (e.g., Constantz, 2008). The relative contribution of advection and conduction to heat transfer can be quantified with the dimensionless Peclet number (Pe) (Silliman et al., 1995):

$$Pe = \frac{v_f \cdot n \cdot l}{D} \tag{12}$$

where l is the characteristic length, set as 0.01 m due to the range of the setup. The thermal diffusivity D is given by:

$$D = \frac{K_e}{c_s \cdot \rho_s} \tag{13}$$

where $K_e$ is the thermal conductivity of the saturated sediment (Table 1). If Pe is smaller than approximately $2 \cdot 10^{-4}$, the advection component of the solution has little impact for fluxes and conductive heat transport dominates (Silliman et al., 1995).

Median Peclet numbers were between approximately 0.01 and 0.1, indicating that heat is transported not only by molecular transport of thermal energy (conduction) but also by water flow (advection) (Silliman et al., 1995).

### 2.6. Groundwater flow modeling

Groundwater flow models for site B were setup in GMS (Groundwater Modeling System 7.1, Environmental Modeling Systems, 2002) on the basis of MODFLOW (McDonald and Harbaugh, 1996). Details can be found in Huber et al. (2013). Boundary conditions of a regional scale groundwater model (extension 230 m × 340 m, resolution 2 m × 2 m) were transferred to an intermediate scale groundwater model (extension 110 m × 60 m, resolution 0.5 m × 0.5 m). For the description of the bedrock surface penetration depth of direct-push boreholes were used. For the intermediate scale model the high-resolution measurements of riverbed morphology were considered. Based on continuously measured groundwater heads, the distribution and magnitude of hydraulic conductivities as well as the riverbed conductance were inversely calibrated for a transient data set (220 days, resolution 1d, PEST, Doherty, 1994).

**Table 1**
Physical parameters used for calculating specific infiltration rates q in alphabetic order (1. Roman letters, 2. Greek letters).

| Symbol | Values | Unit | Parameter |
|---|---|---|---|
| A | | °C | Amplitude of thermal oscillation |
| $A_r$ | | – | Temperature (T) amplitude ratio (upper/lower T amplitude) |
| c | | $J\,kg^{-1}\,°C^{-1}$ | Specific heat of sediment–fluid system |
| $c_f$ | 4208 | $J\,kg^{-1}\,°C^{-1}$ | Specific heat of fluid (water at 4 °C) (Lemmon et al., 2012) |
| $c_s$ | 775 | $J\,kg^{-1}\,°C^{-1}$ | Specific heat of sediments, average between values of Schön (1996) (cited by Rau et al., 2010) and Revil (2000) (cited by Keery et al., 2007) |
| $f_{Day}$ | $11.5 \cdot 10^{-6}$ | $s^{-1}$ | Frequency of a day period (24 h) |
| $K_e$ | 1 | $J\,m^{-1}\,s^{-1}\,K^{-1}$ | Thermal conductivity of the saturated sediment, Carslaw and Jaeger (1959) (cited by Silliman et al., 1995) |
| n | 0.23 | – | Porosity, assessed from freeze core samples |
| q | | $m\,s^{-1}$ | Specific infiltration rate |
| v | | $m\,s^{-1}$ | Velocity of thermal front |
| $v_{Ar}$ | | $m\,s^{-1}$ | Velocity of thermal front derived from the amplitude ratio $A_r$ |
| $v_f$ | | $m\,s^{-1}$ | Vertical fluid velocity, positive number = down welling (Goto et al., 2005) |
| $\beta$ | $1 \cdot 10^{-3}$ | m | Thermal dispersivity (cited by Hatch et al., 2006) |
| $\Delta\phi$ | | s | Temperature amplitude phase shift |
| $\kappa_e$ | | $m^2\,s^{-1}$ | Effective thermal diffusivity |
| $\rho$ | | $kg\,m^{-3}$ | Density of saturated sediment |
| $\rho_f$ | 1000 | $kg\,m^{-3}$ | Density of fluid (water at 4 °C; Kuchling, 1976) |
| $\rho_s$ | 2650 | $kg\,m^{-3}$ | Density of sediment (e.g., Kuntze et al., 1994) |
| $\sigma$ | 1.50 | $W\,m^{-1}\,K^{-1}$ | Thermal conductivity of saturated sediment (Constantz, 2008) |
| $\sigma_f$ | 0.60 | $W\,m^{-1}\,K^{-1}$ | Thermal conductivity of fluid (water; Ingebritsen et al., 2006) |

## 3. Results and discussion

### 3.1. Spatiotemporal changes in riverbed and redd morphology

The riverbed morphology of the Enziwigger changed substantially during high flow events, despite the steps to prevent deep scouring. This was especially true for the two downstream sites B and C (Fig. 2), where flood events in December 2009 triggered river gravel accumulation or scouring up to 0.9 m (Fig. 3). All redds at site B were strongly affected by scouring, while at site C the gravel bed scoured predominately in the pools below steps and accumulated towards the right bank of the river. Sediment displacements varied from terrace to terrace within a site. For example, changes of the riverbed morphology below step 3 at site C were much smaller than at the other two examined steps (Fig. 3, right). This was probably due to the slightly wider riverbed (5.0–5.5 m at step C3, 4.5–5 m at step C2 and 4.5 m at step C1) causing lower water levels and hence less shear stress. These data also agree with the suggestion that sediment transport in rivers is a discontinuous process and sediment often moves in pulses (Klingemann and Emmett, 1982) affected by bed-form and associated sediment sorting (Cudden and Hoey, 2003) or by debris flows (Hoffman and Gabet, 2007). Hence, bed scouring and gravel deposition are not easy predicted, at least on an intermediate scale within individual river sections. Along the entire river (i.e., regional scale) increased gravel displacement was evident at sites B and C as compared to site A (visual interpretation). In total, half of the redds in sites B and C were lost (Fig. 3), while only 8% of the redds were lost at the most upstream site A. This pattern is most likely related to increased bed shear stress in sites B and C caused by higher water levels and only marginally smaller slopes (Schindler Wildhaber et al., 2012b), as also indicated by increasing bedloads and suspended sediment loads from upstream to downstream (Schindler Wildhaber et al., 2012b). In support of this notion the probability of redd excavation increased with the water level above the redd (GLM, $p < 0.05$).

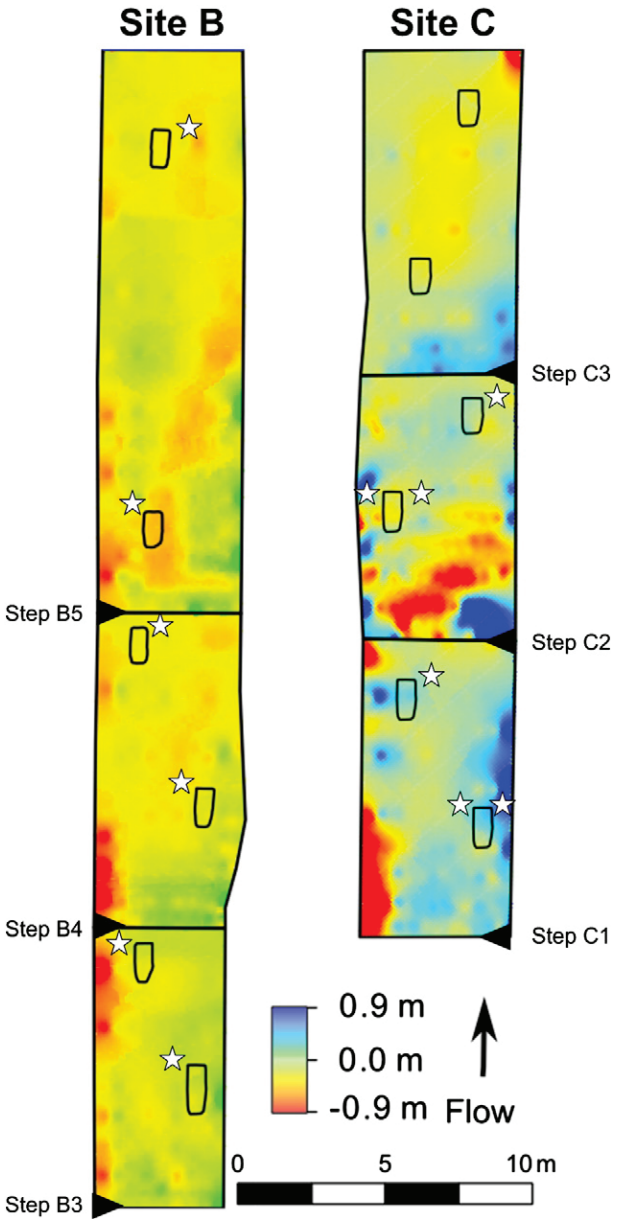


**Fig. 3.** Differences between the riverbed topography measured in October and December 2009 at the two downstream sites B and C. Negative values indicate gravel bed erosion and positive values indicate sediment deposition. Black ovals are the positions of the artificial redds. Redds lost during season 1 are marked by a star on the left side, while redds lost during season 2 are marked by a star on the right side.

Winter flood events in some Swiss rivers and also in rivers worldwide have increased over the last decade (Birsan et al., 2005; Scheurer et al., 2009) and are expected to further increase, both, in respect to intensity and frequency, due to climate change (IPPC, 2007; Middelkoop et al., 2001; Thodsen, 2007). In the Enziwigger, high-flow events in early winter are unusual, but it has been suggested that they have increased in recent decades (P. Amrein, Fish and Wildlife Service, Canton of Lucerne, Switzerland, pers. comm.). Accordingly, the high redd loss reported here raises concerns about how the observed and predicted increases of winter floods affect salmonid recruitment in confined rivers like the Enziwigger with small egg-burial depths (0–9 cm; Riedl and Peter, 2013) making salmonid embryos more susceptible to scouring.

High-flow events also strongly affected the morphology of the remaining redds. Initially, the mean difference between the depth of the tail and pit of newly built redds was $9.4 \pm 2.8$ cm (Fig. 4A). After one month and some high flow events, most redds were basically leveled (Fig. 4A) and a high amount of fine sediment had infiltrated (Schindler Wildhaber et al., 2012b). These observations agree with Ottaway et al. (1981) who documented a flattening of brown trout redds after only the first high water event subsequent to spawning. Both, flattening of the redd and fine sediment content are known to affect the water exchange in redds, either by reducing horizontal pumping flow or by decreasing redd gravel permeability (e.g., Greig et al., 2005; Schälchli, 1995). The concept of enhanced downwelling of oxygenated water due to the redd morphology is still widely discussed (e.g., S.M. Greig et al., 2007; Tonina and Buffington, 2009; Zimmermann and Lapointe, 2005). Our results clearly indicate that redd morphology contributes to local redd scale exchange processes only during the first few weeks after redd building (see below). Once the pit–tail structure has been leveled, exchange processes on intermediate or regional scales gain importance for water-exchange and oxygen supply to developing embryos. In many modified rivers, such processes driven on these scales have to be clearly incorporated into management plans to ensure sufficient salmonid incubation success.

### 3.2. Hydraulic dynamics in the redds

#### 3.2.1. Spatial patterns of the hydraulic dynamics

Vertical hydraulic gradients (VHGs) measured in mini-piezometers did not parallel the expected intermediate scale downwelling and upwelling patterns induced by steps (Gooseff et al., 2006; Huber et al., 2013; Kasahara and Hill, 2006, Fig. 1B). Most redds were located more than one meter before or after a step. Accordingly, they were not located in the main upwelling and downwelling zones predicted by the model, but in areas where downwelling, upwelling and horizontal advection alternate (Fig. 1C). Hence, the applied mini-piezometer approach was

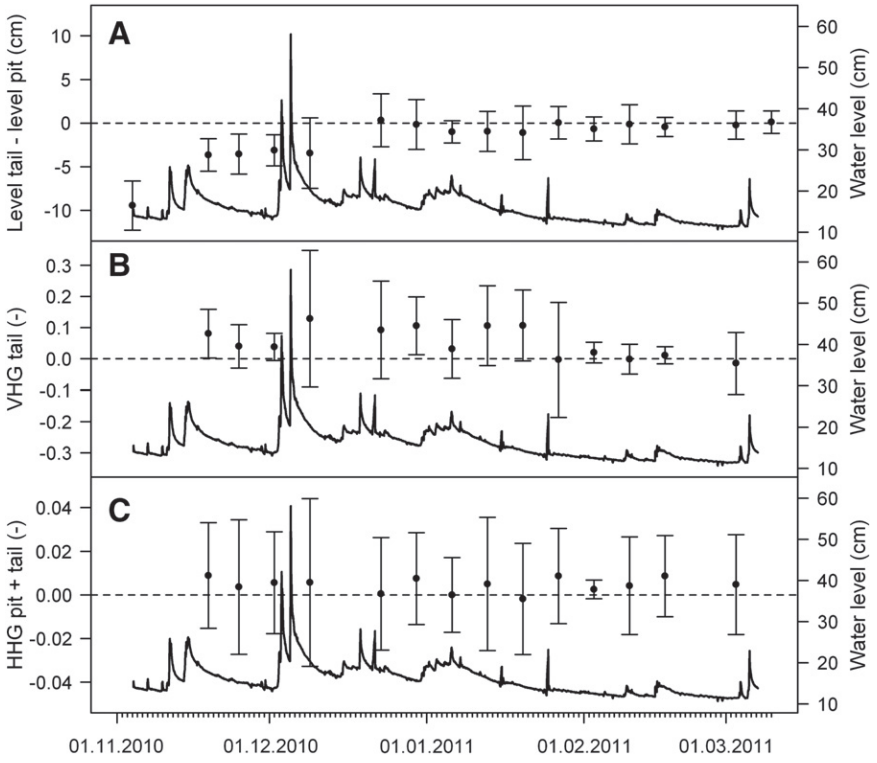


**Fig. 4.** In each panel, the black graph represents the flow stage at site B. Symbols within panels denote (A) the mean ± standard deviation (SD) of the riverbed level differences between tail and pit (B) mean ± SD of the vertical hydraulic gradients (VHGs) in the tail of the redds, and (C) mean ± SD of the horizontal hydraulic gradients (HHGs) between pit and tail of the redds. Values were calculated from all 18 redds during season 2. A positive hydraulic gradient indicates upwelling and a negative gradient indicates downwelling.

most likely not able to integrate the hydraulic gradients that jointly drove water exchange in redds, i.e., both vertical and horizontal. In redd A32_S1, which provides an exception being located only 0.65 m above a step, considerable downwelling potential was measured ($-0.07 \pm 0.06$). When this redd was located 1.65 m upstream of the step in season 2 (redd A32_S2; Fig. 2), VHGs changed between upwelling and downwelling conditions with a mean close to zero ($0.03 \pm 0.08$). This confirms the model predictions. In general, vertical hydraulic gradients on the redd scale can be expected to show substantial temporal variation related to water level fluctuations and also changes in riverbed morphology (cf. Section 3.2.2).

Specific infiltration rates q, calculated from continuous data, confirmed the predictions from the groundwater flow modeling. Mean $q_t$ increased with smaller distance to the next downstream step and hence confirmed the increased downwelling above steps (Table 2). Similarly, in redds located further upstream smaller and also negative $q_t$ values were found, which again agrees with model predictions (Fig. 1C). Also, weekly fine sediment infiltration increased with shorter distance to the downstream step (Spearman rank correlation, fine sediment: $\rho = -0.45$, $p < 0.05$, silt: $\rho = -0.52$, $p < 0.05$, clay: $\rho = -0.57$, $p < 0.01$), likely related to increased river water infiltration above steps. Increased weekly fine sediment infiltration had no negative effect on specific water infiltration in redds (Table 2). However, the net fine sediment accumulation did not increase with shorter distance to the step (all $p > 0.12$). Fine sediment accumulation depends not only on fine sediment infiltration, but also on water level, since higher water levels lead to resuspension of fine sediment (see also Schindler Wildhaber et al., 2012b). The specific infiltration rate q decreased significantly in redds with higher fine sediment accumulation and increased with a higher maximal water level above the redd (Table 2).

**Table 2**
Spearman rank correlations between median specific infiltration rate q in the upper part (0–12 cm; $q_u$) and the total part (0–20 cm, $q_t$) and the total amount of accumulated fine sediment (<2 mm), the accumulated silt and clay fraction, the sum of weekly infiltrated fine sediment, the Fredle index of the accumulation baskets, the maximal water level above the redd and the distance of the redd to the upstream and downstream step. Sample size (n) is given in parentheses.

| | $q_u$ ($m\,s^{-1}$) | $q_t$ ($m\,s^{-1}$) |
|---|---|---|
| Fine sediment accu. (%) | −0.79, p = 0.03 (8) | −0.89, p = 0.03 (6) |
| Silt and clay accu. (%) | −0.52, p = 0.20 (8) | −0.49, p = 0.36 (6) |
| Fine sediment infiltration (g) | −1.9, p = 0.58 (8) | −0.18, p = 0.57 (6) |
| Fredle index (−) | 0.71, p = 0.06 (8) | 0.77, p = 0.09 (6) |
| Water max. (cm) | 0.60, p = 0.03 (13) | 0.66, p = 0.03 (10) |
| Distance upstream step (cm) | 0.15, p = 0.62[a] (13) | 0.61, p = 0.06[a] (10) |
| Distance downstream step (cm) | −0.17, p = 0.58[a] (13) | −0.68, p = 0.03[a] (10) |

[a] Mean q of February and March to get a mean q value of the undisturbed river gravel.

Hydraulic exchange processes can vary remarkably within a single redd. In most redds q was lower in 12–20 cm depth as compared to the upper 12 cm of redd gravel (t-test, $p < 0.01$; Fig. 5). Freeze core samples of undisturbed gravel in the study area confirmed a significantly lower silt and clay level in the upper part (0–10 cm) compared to the deeper part (i.e., 10–20 cm and 20–30 cm, cf. Schindler Wildhaber et al., 2012b). A comparable increase in fine sediment content paralleled by a decreased hydraulic conductivity was also found in the studies of Brunke (1999) and Sear (1993). Accordingly, the decrease of q with depth reported here suggests higher fine sediment content around our brown trout eggs (i.e., at 12–20 cm depth) compared with the entire redd gravel. A similar distinction between the upper and lower part of the redd gravel was made by Meyer (2003). Our study further documents that this increased fine sediment accumulation around the eggs can decrease water exchange around the eggs, which could hinder oxygen supply to the embryos (see Section 3.3.2) and hence salmonid embryo survival.

At redd A32_S1, the specific infiltration q was higher in the bottom part than the upper part of the redd (Fig. 5, see Fig. 2 for location of the redd), which was probably related to the lower mean water level above this redd ($9.8 \pm 2.0$ cm), triggering high fine sediment deposition and only limited scouring (Schindler Wildhaber et al., 2012b). Redd

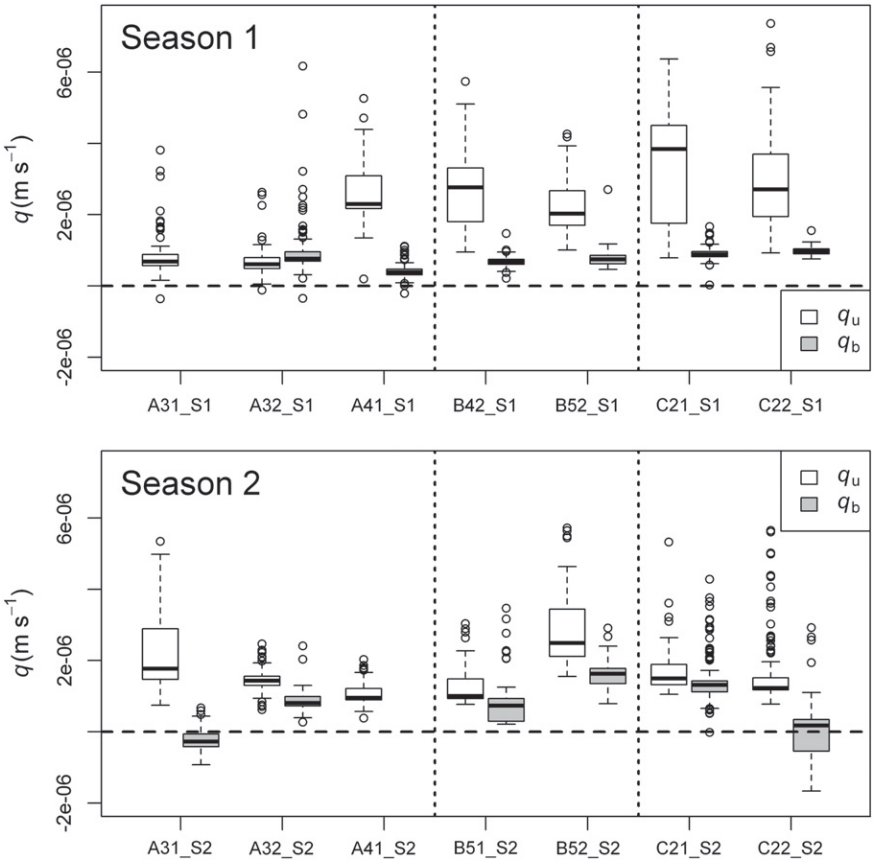


**Fig. 5.** Specific water infiltration rates in the upper ($q_u$) and the bottom part ($q_b$) of the redds during season 1 (top) and season 2 (bottom). Negative values indicate upwelling, positive values indicate downwelling. For each redd the horizontal line indicates the median, the box interquartile range (i.e., center 50% of the data), whiskers mark maximum and minimum values, and points denote values exceeding 1.5 times the interquartile range. Among seasons, redds were built in the same location (Fig. 2) with the exception of redds A31 and A32 (see Section 3.2.1).

A32_S1 was also the only redd equipped with temperature probes that was temporally covered with ice, which could have caused decreased water flow over the redd. In addition, VHG measurements indicated substantial downwelling potential in this redd (VHG $= -0.07 \pm 0.06$, see above). Both factors possibly increased the fine sediment input in the entire gravel column of this redd (Brunke, 1999; Schindler Wildhaber et al., 2012b; Seydell et al., 2009) and hence decreased specific water infiltration q also in the upper part. A low q was also found in the upper part of redd A31_S1 (Fig. 5), which also had a very low mean water level ($2.5 \pm 1.7$ cm). During the second field season, the locations of two redds were changed to locations with deeper mean water levels (A31_S2: $15.1 \pm 3.5$ cm, A32_S2: $12.4 \pm 3.5$ cm). This resulted in less fine sediment accumulation (Schindler Wildhaber et al., 2012b) and higher specific infiltration rates q were found (Fig. 5). Further, these patterns of q were closely paralleled by the oxygen dynamics in these redds (see Section 3.3.2).

*3.2.2. Temporal pattern of the hydraulic dynamics*

Slightly positive VHGs, indicating upwelling processes, were measured in the tail of most redds at the beginning of the incubation period (Fig. 4B). In contrast, horizontal hydraulic gradients (HHGs) between pit and tail did not indicate increased horizontal pumping flows between pit and tail (Fig. 4C). The often suggested redd scale flow pattern, with downwelling in the pit and upwelling in the tail (Tonina and Buffington, 2009), was therefore not confirmed by the HHG measurements. One reason for this might be the influence of the riverbed morphology or the water levels on the vertical and horizontal hydraulic gradients, as indicated by significant correlations between VHGs and the water level ($\rho = 0.4$–$0.6$, $p < 0.05$ in 8 of the 18 redds, Fig. 6).

During base flow, VHGs were mostly negative or around zero, indicating downwelling or horizontal advection flow, which agrees with model predictions (Huber et al., 2013). Upwelling or lateral flow dominated for VHG values measured at higher water levels (Fig. 6). On an intermediate scale, upwelling increases below steps (Gooseff et al., 2006; Huber et al., 2013; Kasahara and Hill, 2006). On a regional scale, upwelling can occur when increasing riparian groundwater levels are paralleled by decreasing stream water levels, e.g., during the recession limb of flood events (Geist et al., 2008; Malcolm et al., 2003, 2006; Soulsby et al., 2009). In the Enziwigger, VHG measurements during the rising limb or flood events were not possible because of dangerous physical conditions. Most of the higher water levels in Fig. 6 therefore represent data points measured during the recession limb of flood events. Therefore, the positive hydraulic gradients (Fig. 6) indicate most likely recharge of groundwater on a regional scale and related upwelling in the redds.

Hyporheic flow paths in rivers can be very complex and also change with discharge and morphology (Tonina and Buffington, 2007). In our study, these complex temporal dynamics can best be seen in the specific water infiltration rates. Initially, q values in most redds were consistently high ($6$–$7 \cdot 10^{-6}$ m s$^{-1}$), and decreased markedly within a month – likely related to fine sediment accumulation and changes in redd morphology – to finally stabilize around $1$–$2 \cdot 10^{-6}$ m s$^{-1}$ for the rest of the incubation season (Figs. 7, 5). Nonetheless, on the scale of hours and days, q remained responsive to water-level fluctuations, when it increased during high-flow events and returned to baseline levels afterwards (Fig. 7). The most likely explanation for this are local changes in groundwater heads in combination with increased gravel permeability related to remobilization of fine sediment (e.g., Brunke, 1999; Keery et al., 2007; Schälchli, 1995).

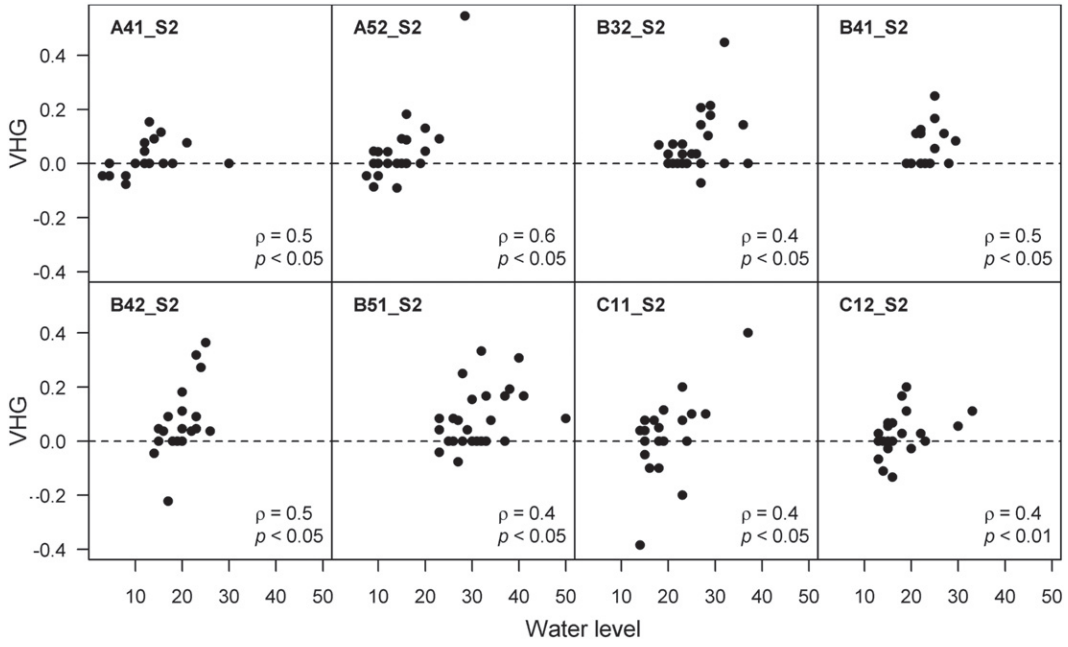


**Fig. 6.** Relationship between water level and vertical hydraulic gradient (VHG) for individual redds from season 2. Within each panel Spearman correlation coefficient rho (ρ) and the p-value are given. Positive VHG indicates upwelling, and negative VHG indicates downwelling. The location of each redd is given in Fig. 2.

Temporally negative q values, and hence upwelling were found in the bottom part (approx. 12–20 cm) of two redds (A31_S2 and C22_S2) where consistent downwelling occurred in the upper part (Fig. 5). Redd C22 (Fig. 8) was located just above a step, where downwelling predominates (Huber et al., 2013). Further, it was located on the right side of the Enziwigger, close to a small tributary river driving exfiltration of groundwater (Fig. 2). Given this specific location, we suspect that river water infiltrated in the upper part of this redd (positive q), while groundwater exfiltrated into the lower part (negative q). As discussed above, this groundwater exfiltration increased during the recession limb of high flow events (Fig. 8). Altogether, these data clearly indicate that exchange processes in salmonid redds are driven on different scales, and that these processes altogether determine water-exchange patterns in the egg pocket, which will then have an influence on the likelihood of embryo survival (Michel et al., in revision).

Specific water infiltration rates q calculated with the intermediate groundwater flow model for specific redd locations in downwelling zones ranged between $8.5 \cdot 10^{-7}$ and $1.5 \cdot 10^{-5}$ m s$^{-1}$ (season 1, Huber et al., 2013). Measured daily $q_t$ values at redd B42_S1 correlated with the modeled values (Pearson's $r = 0.3$, $p < 0.05$). At redd B52_S1, no significant correlation was found. The groundwater flow model was set up using hydraulic heads of the river and groundwater as well as the local and regional topography. In contrast, the actual q in the redds further depends on the hydraulic conductivity, affected by fine sediment deposition and hydraulic gradients on the redd scale. These differences could have contributed to the lack of correlation in the latter redd, since water exchange rates on the redd scale can vary strongly, either depending on reach scale bedform character and barriers (Baxter and Hauer, 2000) or differences in hydraulic conductivities (Brunke and Gonser, 1997). These results indicate that groundwater flow modeling as applied in Huber et al. (2013) can predict exchange processes on the regional and intermediate scales, but is limited in predicting exchange processes on the redd scale.

Altogether, these findings illustrate that water exchange processes in salmonid redds are complex and driven on multiple scales. Consequently, fine sediment effects on salmonid embryo survival can be expected to differ depending on the redd location relative to river

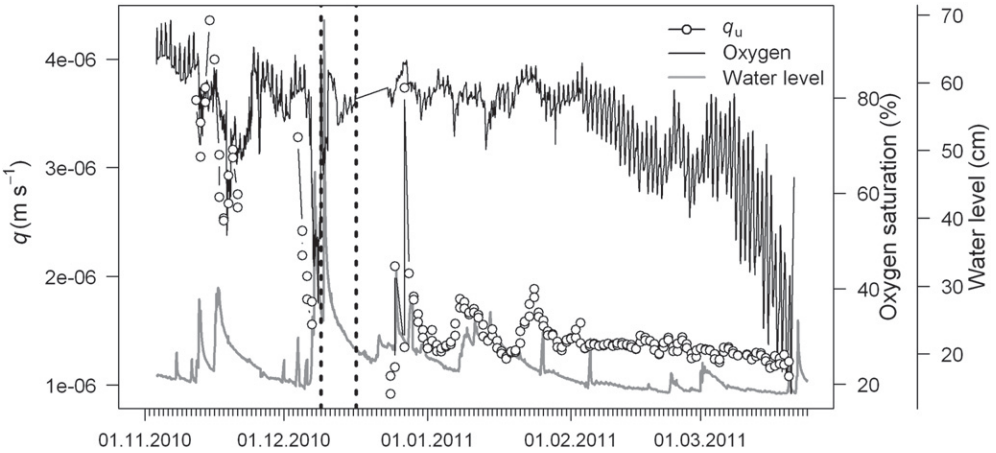


**Fig. 7.** Example of the temporal dynamics of the specific infiltration q in the upper part of the redd gravel ($q_u$), the oxygen concentration and the water level. Shown are data from redd C21_S2 (cf. Fig. 2). A period when oxygen and temperature probes were dug out is marked with vertical dashed lines.

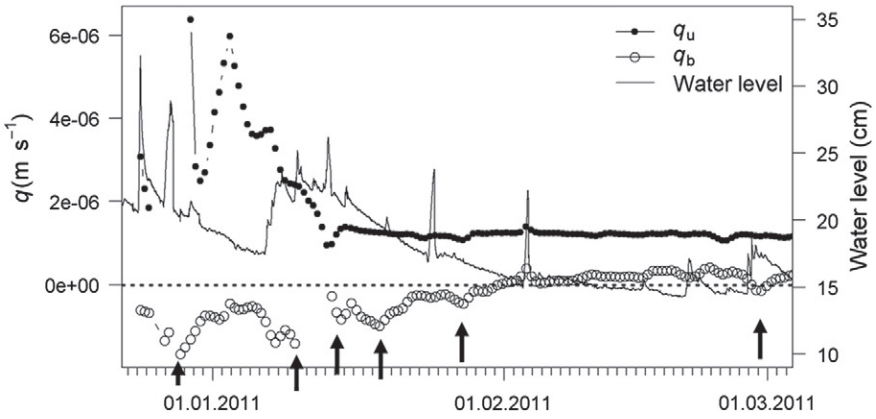


**Fig. 8.** Temporal changes of the specific infiltration rate q in the upper and the bottom part of the redd C22_S2 (cf. Fig. 2 for location of the redd). Negative values indicate upwelling, positive values indicate downwelling. The arrows point to periods with increased upwelling during the falling limb of high flow events.

morphology and structure and also on regional aspects, such as river interactions with the valley aquifer.

### 3.3. Oxygen

#### 3.3.1. Manual vs. continuous oxygen measurements

Manual oxygen measurements, conducted on bi-weekly intervals during season 2 in mini-piezometers, indicated a high interstitial dissolved oxygen (DO) concentration in the redds (10.1 ± 2.2 mg $l^{-1}$/75.7 ± 15.7%). However, DO concentrations measured manually did not correlate with DO concentrations from permanent oxygen measurements. Oxygen concentrations in salmonid redds can vary substantially with time (Heywood and Walling, 2007, this study), and hence even weekly or bi-weekly measuring intervals have a high risk of underestimating extreme values (Malcolm et al., 2006). Manual measurements in piezometers could therefore over- or underestimate the amount of oxygen present in salmonid redds, being a poor descriptor for oxygen dynamics during the incubation season. Given these limitations and the methodological bias of the manual DO data, further interpretations are based only on the continuous DO measurements.

#### 3.3.2. Spatial oxygen dynamics

Dissolved oxygen concentrations from continuous measurements in redds documented a high variability on small spatial scales (i.e., between redds), but also a general increase from upstream to downstream (Table 3). Interstitial oxygen concentrations at site A (redd A32_S1) were especially low during season 1 with DO concentrations below 3 mg $l^{-1}$ during 44 of total 135 days of egg incubation time. A DO concentration of 3 mg $l^{-1}$ is considered as a critical threshold for salmonid embryo survival (Michel et al., in revision). The low DO concentrations in this redd could be related to low specific water infiltration q (see Section 3.2.1). This is supported by the observation that, when this redd was moved to a location with a higher water level during season 2, not a single day below 3 mg $l^{-1}$ occurred (redd A32_S2; Table 3). In contrast, redd A31_S2, built about six meters upstream of A32_S2, had 14 days with DO concentrations below 3 mg $l^{-1}$, likely related to upwelling of DO depleted hyporheic water, as discussed in Section 3.2.2 (Fig. 5). Days below 3 mg $l^{-1}$ were far less frequent at sites B and C (Table 3). These observed low oxygen concentrations at site A could be related to the artificial log steps, breaking down the river slope, inhibiting natural river gravel movements and thus triggering high fine sediment accumulation at sites with low water levels. At the downstream sites, water levels and shear stress were generally higher, leading to a flushing of infiltrated fine sediment, and less accumulation (Schindler Wildhaber et al., 2012b).

Only a small number of accumulation baskets in redds with permanent oxygen measurements survived floods, resulting in a very small data set (n = 4) across the two field seasons (Schindler Wildhaber et al., 2012b). However, these four data points were surprisingly evenly spread and showed a perfect linear decrease of the mean DO concentration with increasing fine sediment accumulation (Fig. A1). This has been repeatedly demonstrated before (e.g., Heywood and Walling, 2007), and indicates that also in our study river increased fine sediment accumulation could negatively affect embryo survival by decreasing oxygen supply.

#### 3.3.3. Temporal oxygen dynamics

On the scale of hours and days, DO concentrations decreased during the falling limb of high flow events. This pattern was most pronounced when temporal water exfiltration was measured, e.g., redd A31_S2 (Fig. 9, see also Section 3.2.2), and thus most likely related to intermittent exfiltration of depleted groundwater or hyporheic water through the redd (Section 3.2.2). The same has been reported in other studies (Malcolm et al., 2010, 2006; Soulsby et al., 2009). Nonetheless, decreasing DO concentrations during the falling limb of high flow events were also found in locations where no exfiltration was measured (e.g., redd C21_S2, Fig. 7). Here interstitial DO quickly returned to normal levels after the rising limb of high flow events, also suggesting that this pattern is related to groundwater exfiltration rather than increased fine sediment deposition, which would have likely caused more prolonged effects (Fig. 7).

**Table 3**
Mean oxygen concentrations calculated from continuous measurement with permanent oxygen probes in one redd per site during season 1 (S1) and two redds per site during season 2 (S2). Given are mean ± standard deviations, minimum (min) and number of days wherein oxygen concentration was below 3 mg $l^{-1}$.

| Site | Mean ± SD $O_2$ (mg $l^{-1}$) | | | Min $O_2$ | | Days $O_2$ < 3 mg $l^{-1}$ | |
|---|---|---|---|---|---|---|---|
| | S1 | S2 | Mean (S1 + S2) | S1 | S2 | S1 | S2 |
| A | 4.6 ± 3.3 | 8.4 ± 3.4 | 6.6 ± 3.8 | 0.0 | 0.1 | 44 | 14\|0 |
| B | 9.6 ± 2.1 | 10.0 ± 2.3 | 9.8 ± 2.2 | 3.2 | 0.0 | 0 | 4\|2 |
| C | 9.6 ± 1.8 | 10.3 ± 1.3 | 10.0 ± 1.6 | 0.6 | 3.8 | 1 | 1\|0 |

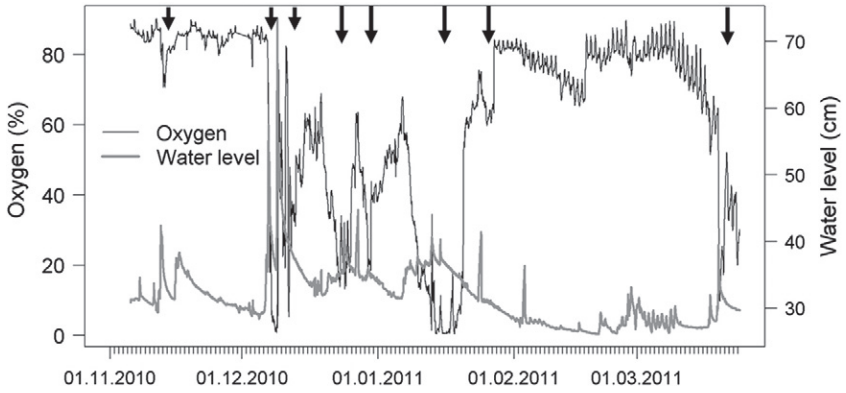


**Fig. 9.** Example for temporal oxygen concentration and water level dynamics (redd A31_S2, cf. Fig. 2 for location of the redd). Arrows mark the decrease of oxygen concentrations during the falling limb of high flow events.

In addition to these changes in interstitial DO on the scale of hours and days, two general trends over the entire incubation period were evident. The first trend could be observed at the beginning of the incubation season: shortly after redd construction, DO was generally high and paralleled by high specific water infiltration rates q (10–12 mg $l^{-1}$, or 80–90% oxygen saturation; for an example see Fig. 7). Within a few weeks, interstitial DO decreased in parallel with q, as also reflected in significant correlations between these two parameters (Fig. 10). The different forms of this relationship among redds (Fig. 10) could be related to local conditions at the redd location that also affect interstitial DO (e.g., organic content, groundwater influence). The second trend could be observed at the end of the incubation season, when several redds showed a distinct decrease in interstitial oxygen during spring, i.e., just before hatching (Figs. 7, 9). This decrease was usually preceded by prolonged periods of base flow, when smaller sediment particles infiltrated in the redds (Schindler Wildhaber et al., 2012b). These silt and clay sized particles can effectively induce siltation of the riverbed, thereby decreasing hydraulic conductivity (Schälchli, 1995). Moreover, the organic matter concentration of the infiltrated fine sediment increased during base flow conditions (Schindler Wildhaber et al., 2012a). Together with rising water temperatures during spring, the latter likely further decreased the oxygen concentration in the redds (S.M. Greig et al., 2007). This decrease towards the time of hatching, when oxygen demand of the salmonid embryos is at maximum (S.M. Greig et al.,

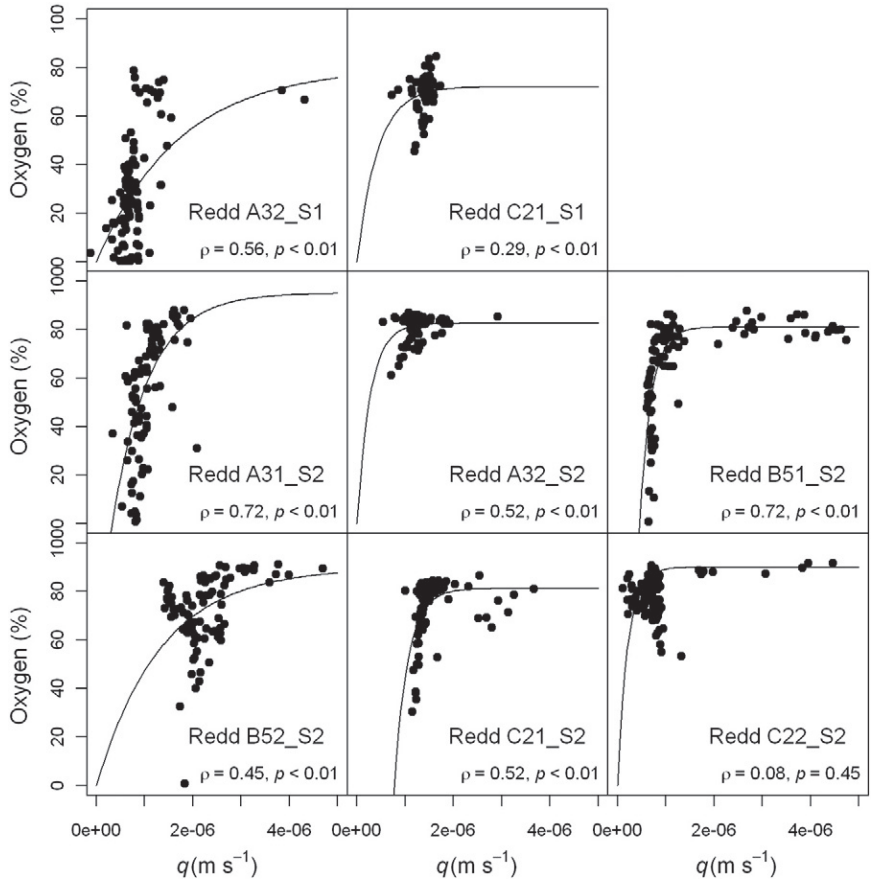


**Fig. 10.** Relationships between the mean daily oxygen concentrations in redds and the specific infiltration rates $q_t$ with non-linear regression lines. Within each panel Spearman correlation coefficient rho (ρ) and the p-value are given. See Fig. 2 for location of the redds.

2007), might have also affected embryo survival in some redds (Michel et al., in revision).

## 4. Conclusion

Artificial steps in channelized rivers can have positive or negative effects on incubating salmonid embryos. In downstream sections, where canalization of the riverbed cause higher water level and an increased slope, resulting in a higher sediment transport capacity, artificial steps decrease river gravel movements and thus scouring of the riverbed. Additionally, artificial steps increase hyporheic exchange processes. Further upstream, in low flow sections, where slopes would naturally be higher, artificial steps inhibit natural river gravel movements due to the decreased riverbed slope. This triggers higher fine sediment infiltration and accumulations, resulting in lower specific water infiltration rates (q) and hyporheic oxygen.

Our data further more demonstrate that q and dissolved oxygen (DO) concentrations in salmonid redds are highly dynamic and driven on multiple scales. Clearly, q and interstitial DO in salmonid redds are affected by conditions at the redd location, such as the amount of accumulated fine sediment, organic content and redd morphology. However, local factors of the magnitude of centimeters to meters are regularly superimposed by processes driven on the intermediate scale (in the range of meters) and regional scale (in the range of tenths of meters to kilometers). On an intermediate scale artificial steps can affect patterns of fine sediment accumulation, water exchange in salmonid redds and hence interstitial DO.

Our results document for the first time an effect of artificial steps on water exchange and oxygen concentrations in salmonid redds. Given the complex interaction of all the processes studied here, multiple factors have to be considered to predict salmonid embryo survival, which is highly time and work intensive. Multiple predictors should include oxygen and fine sediment measurements, riverbed structure such as artificial steps or the channelized riverbed and the hydrological setting of the river in the valley aquifer.

Supplementary data to this article can be found online at http://dx.doi.org/10.1016/j.scitotenv.2013.09.100.

## Acknowledgments

This study was funded by the Swiss National Science Foundation (SNSF projects K-32K1-120486 and CR23I2_138025). We thank Sandra Rudolf, Bastian Brun and Annina Gysel for their help in the field, Marianne Caroni and Ruth Strunk for their laboratory assistance and measurements, Johannes Fritsche for his help with R analyses and Claude Schneider and Lukas Zimmermann for their technical support. The corrections of Andrew Clarke improved language and grammar of the manuscript, thank you. Finally, we greatly acknowledge the extensive support of Phillip Amrein (Fish and Wildlife Service, Canton Lucerne, Sursee, Switzerland).

## References

Acornley RM, Sear DA. Sediment transport and siltation of brown trout (*Salmo trutta* L.) spawning gravels in chalk streams. Hydrol Process 1999;13:447–58.
Baxter CV, Hauer FR. Geomorphology, hyporheic exchange, and selection of spawning habitat by bull trout (*Salvelinus confluentus*). Can J Fish Aquat Sci 2000;57:1470–81.
Baxter C, Hauer FR, Woessner WW. Measuring groundwater–stream water exchange: new techniques for installing minipiezometers and estimating hydraulic conductivity. Trans Am Fish Soc 2003;132:493–502.
Birsan MV, Molnar P, Burlando P, Pfaundler M. Streamflow trends in Switzerland. J Hydrol 2005;314:312–29.
Brookes A. Channelized rivers: perspectives for environmental management. Chichester: Wiley; 1988.
Brown LR, Moyle PB, Yoshiyama RM. Historical decline and current status of coho salmon in California. N Am J Fish Manag 1994;14:237–61.
Brunke M. Colmation and depth filtration within streambeds: retention of particles in hyporheic interstices. Int Rev Hydrobiol 1999;84:99–117.
Brunke M, Gonser T. The ecological significance of exchange processes between rivers and groundwater. Freshw Biol 1997;37:1–33.
Burkhardt-Holm P, Scheurer K. Application of the weight-of-evidence approach to assess the decline of brown trout (*Salmo trutta*) in Swiss rivers. Aquat Sci 2007;69:51–70.
Carslaw HS, Jaeger JC. Conduction of heat in solids. New York: Oxford University; 1959.
Constantz J. Heat as a tracer to determine streambed water exchanges. Water Resour Res 2008;44.
Crisp DT, Carling PA. Observations on siting, dimensions and structure of salmonid redds. J Fish Biol 1989;34:119–34.
Cudden JR, Hoey TB. The causes of bedload pulses in a gravel channel: the implications of bedload grain-size distributions. Earth Surf Process Landf 2003;28:1411–28.
Doherty J. PEST model—independent parameter estimation. Corinda, Australia.: Watermark Computing; 1994
EBP-WSB-Agrofutura. Ganzheitliche Gewässerplanung im Einzugsgebiet Wiggertal. Bau- und Umwelt und Wirtschaftsdepartement des Kantons Luzern und Baudepartement des Kantons Aargau; 2005.
Endreny T, Lautz L, Siegel DI. Hyporheic flow path response to hydraulic jumps at river steps: flume and hydrodynamic models. Water Resour Res 2011;47.
Environmental Modeling Systems I. GMS: Groundwater Modeling System; 2002 [South Jordan, Utah].
Geist DR, Arntzen EV, Murray CJ, McGrath KE, Bott YJ, Hanrahan TP. Influence of river level on temperature and hydraulic gradients in chum and fall Chinook salmon spawning areas downstream of Bonneville Dam, Columbia river. N Am J Fish Manag 2008;28:30–41.
Gilvear DJ, Heal KV, Stephen A. Hydrology and the ecological quality of Scottish river ecosystems. Sci Total Environ 2002;294:131–59.
Gooseff MN, Anderson JK, Wondzell S, LaNier J, Haggerty R. A modeling study of hyporheic exchange pattern and the sequence, size, and spacing of stream bedforms in mountain stream networks, Oregon, USA (retraction of vol 19, pg 2915, 2005). Hydrol Process 2006;20:2443–57.
Goto M, Matsukara N, Hagiwara Y. Heat transfer characteristics of warm water flow with cool immiscible droplets in a vertical pipe. Exp Thermal Fluid Sci 2005;29:371–81.
Greig SM, Sear DA, Carling PA. The impact of fine sediment accumulation on the survival of incubating salmon progeny: implications for sediment management. Sci Total Environ 2005;344:241–58.
Greig S, Sear D, Carling P. A field-based assessment of oxygen supply to incubating Atlantic salmon (*Salmo salar*) embryos. Hydrol Process 2007a;21:3087–100.
Greig SM, Sear DA, Carling PA. A review of factors influencing the availability of dissolved oxygen to incubating salmonid embryos. Hydrol Process 2007b;21:323–34.
Hatch CE, Fisher AT, Revenaugh JS, Constantz J, Ruehl C. Quantifying surface water–groundwater interactions using time series analysis of streambed thermal records: method development. Water Resour Res 2006;42.
Heywood MJT, Walling DE. The sedimentation of salmonid spawning gravels in the Hampshire Avon catchment, UK: implications for the dissolved oxygen content of intragravel water and embryo survival. Hydrol Process 2007;21:770–88.
Hicks BJ, Hall JD, Bisson PA, Sedell JR. Responses of salmonids to habitat changes. In: Meehan WR, editor. Influences of forest and rangeland management on salmonid fishes and their habitats, 19. ; 1991. p. 483–518.
Hoffman DE, Gabet EJ. Effects of sediment pulses on channel morphology in a gravel-bed river. Geol Soc Am Bull 2007;119:116–25.
Huber E, Huggenberger P, Epting J, Schindler Wildhaber Y. Zeitliche und räumliche Skalen der Fluss–Grundwasser Interaktion: ein multidimensionaler hydrogeologischer Untersuchungsansatz — spatiotemporal scales of river–groundwater interaction: a multidimensional hydrogeoligical investigation approach. Grundwasser 2013;18:159–72.
Hütte M, Niederhauser P. Ökomorphologie Stufe F. Methoden zur Untersuchung und Beurteilung der Fliessgwässer in der Schweiz. Bundesamt für Umwelt, Wald und Landschaft, Mitteilungen zum Gewässerschutz; 199827.
Ingebritsen S, Sanford W, Neuzil C. Groundwater in geologic processes. New York: Cambridge University Press; 2006.
IPPC. Climate change 2007: the physical science basis, summary for policymakers. Intergovernmental panel on climate change; 2007.
Jensen DW, Steel EA, Fullerton AH, Pess GR. Impact of fine sediment on egg-to-fry survival of Pacific salmon: a meta-analysis of published studies. Rev Fish Sci 2009;17:348–59.
Kasahara T, Hill AR. Hyporheic exchange flows induced by constructed riffles and steps in lowland streams in southern Ontario, Canada. Hydrol Process 2006;20:4287–305.
Keery J, Binley A, Crook N, Smith JWN. Temporal and spatial variability of groundwater–surface water fluxes: development and application of an analytical method using temperature time series. J Hydrol 2007;336:1–16.
Klingemann PC, Emmett WW. Gravel bedload transport processes. In: Hey RD, Bathurst JC, Thorne CR, editors. Gravel-bed rivers. Chichester: Wiley; 1982. p. 145–69.
Kuchling H. Taschenbuch der Physik. Verlag Harri Deutsch: Thun; 1976.
Kuntze H, Roeschmann G, Schwerdtfeger G. Bodenkunde. Stuttgart: Ulmer UTB für Wissenschaft; 1994.
Lemmon EW, McLinden MO, Friend DG. "Thermophysical properties of fluid systems" in NIST Chemistry WebBook, NIST Standard Reference Database number 69, Eds. P.J. Linstrom and W.G. Mallard, National Institute of Standards and Technology, Gaithersburg MD, 20899, http://webbook.nist.gov, retrieved February 1, 2012.
Lotspeich FD, Everest FH. A new method for reporting and interpreting textural composition of spawning gravel. In: Service USF, editor. Pacific Northwest Research note PNW-369; 1981. (12 pp.).
Malcolm IA, Youngson AF, Soulsby C. Survival of salmonid eggs in a degraded gravel-bed stream: effects of groundwater–surfacewater interactions. River Res Appl 2003;19:303–16.
Malcolm IA, Soulsby C, Youngson AF. High-frequency logging technologies reveal state-dependent hyporheic process dynamics: implications for hydroecological studies. Hydrol Process 2006;20:615–22.

Malcolm IA, Greig SM, Youngson AF, Soulsby C. Hyporheic influences on salmon embryo survival and performance. Salmonid spawning habitat in riversPhysical controls, biological responses, and approaches to remediation, 65; 2008225–48.
Malcolm IA, Soulsby C, Youngson AF, Tetzlaff D. Fine scale variability of hyporheic hydrochemistry in salmon spawning gravels with contrasting groundwater–surface water interactions. Hydrogeol J 2009;17:161–74.
Malcolm IA, Middlemas CA, Soulsby C, Middlemas SJ, Youngson AF. Hyporheic zone processes in a canalised agricultural stream: implications for salmonid embryo survival. Fundam Appl Limnol 2010;176:319–36.
McDonald MG, Harbaugh AW. Programmer's documentation for MODFLOW-96, an update to the U.S. Geological Survey modular finite-difference ground-water flow model. U.S. Geological Survey open-file report. Reston: U.S. Geological Survey; 1996. p. 96-486.
Meyer CB. The importance of measuring biotic and abiotic factors in the lower egg pocket to predict coho salmon egg survival. J Fish Biol 2003;62:534–48.
Michel C., Schindler Wildhaber Y., Epting J., Thorpe K.L., Huggenberger P., Alewell C. and Burkhardt-Holm P. Artificial steps mitigate fine sediment effects on brown trout embryo survival in a heavily modified river. Journal of Freshwater Biology in revision.
Middelkoop H, Daamen K, Gellens D, Grabs W, Kwadijk JCJ, Lang H, et al. Impact of climate change on hydrological regimes and water resources management in the Rhine basin. Clim Change 2001;49:105–28.
Newson M, Sear D, Soulsby C. Incorporating hydromorphology in strategic approaches to managing flows for salmonids. Fish Manag Ecol 2012;19:490–9.
Ottaway EM, Carling PA, Clarke A, Reader NA. Observations on the structure of brown trout, *Salmo trutta* Linnaeus, redd. J Fish Biol 1981;19:593–607.
Rau GC, Andersen MS, McCallum AM, Acworth RI. Analytical methods that use natural heat as a tracer to quantify surface water–groundwater exchange, evaluated using field temperature records. Hydrogeol J 2010;18:1093–110.
Revil A. Thermal conductivity of unconsolidated sediments with geophysical applications. Geophys Res Solid Earth 2000;105:16749–68.
Riedl C, Peter A. Timing of brown trout spawning in Alpine rivers with special consideration of egg burial depth. Ecol Freshw Fish 2013:1–14.
Sawyer AH, Cardenas MB, Buttles J. Hyporheic exchange due to channel-spanning logs. Water Resour Res 2011:47.
Schager E, Peter A, Burkhardt-Holm P. Status of young-of-the-year brown trout (*Salmo trutta* fario) in Swiss streams: factors influencing YOY trout recruitment. Aquat Sci 2007;69:41–50.
Schälchli U. Basic equations for siltation of riverbeds. J Hydraul Eng ASCE 1995;121:274–87.
Scheurer K, Alewell C, Bänninger D, Burkhardt-Holm P. Climate and land-use changes affecting river sediment and brown trout in alpine countries — a review. Environ Sci Pollut Res 2009;16:232–42.
Schindler Wildhaber Y, Liechti R, Alewell C. Organic matter dynamics and stable isotope signature as tracers of the sources of suspended sediment. Biogeosciences 2012a;9:1985–96.
Schindler Wildhaber Y, Michel C, Burkhardt-Holm P, Bänninger D, Alewell C. Measurement of spatial and temporal fine sediment dynamics in a small river. Hydrol Earth Syst Sci 2012b;16:1501–15.
Schön J. Physical properties of rocks: fundamentals and principles of petrophysics — handbook of geophysical exploration. New York: Pergamon; 1996.
Sear DA. Fine sediment infiltration into gravel spawning beds within a regulated river experiencing floods — ecological implications for salmonids. Regul Rivers Res Manag 1993;8:373–90.
Sear DA, Frostick LB, Rollinson G, Lisle TE. The significance and mechanics of fine-sediment infiltration and accumulation in gravel spawning beds. Am Fish Soc Symp 2008;65:149–73.
Seydell I, Ibisch RB, Zanke UCE. Intrusion of suspended sediments into gravel riverbeds: influence of bed topography studied by means of field and laboratory experiments. Adv Limnol 2009;61:67–85.
Silliman SE, Ramirez J, McCabe RL. Quantifying downflow through creek sediments using temperature time-series — one-dimensional solution incorporating measured surface-temperature. J Hydrol 1995;167:99–119.
Soulsby C, Malcolm IA, Tetzlaff D, Youngson AF. Seasonal and inter-annual variability in hyporheic water quality revealed by continuous monitoring in a salmon spawning stream. River Res Appl 2009. http://dx.doi.org/10.1002/rra.1241.
Sponagel H, Grottenthaler W, Hartmann K-J, Hartwich R, Janetzko P, Joisten H, et al. Bodenkundliche K.artieranleitung. Hannover: Bundesanstalt für Geowissenschaften und Rohstoffe; 2005.
Stucki P. Methoden zur Untersuchung und Beurteilung der Fliessgwässer. Makrozoobenthos Stufe F, Umwelt-Vollzug. Bern: Bundesamt für Umwelt; 2010, 1027.
Thodsen H. The influence of climate change on stream flow in Danish rivers. J Hydrol 2007;333:226–38.
Tonina D, Buffington JM. Hyporheic exchange in gravel bed rivers with pool-riffle morphology: laboratory experiments and three-dimensional modeling. Water Resour Res 2007;43:16.
Tonina D, Buffington JM. A three-dimensional model for analyzing the effects of salmon redds on hyporheic exchange and egg pocket habitat. Can J Fish Aquat Sci 2009;66:2157–73.
Wohl E. Human impacts to mountain streams. Geomorphology 2006;79:217–48.
Youngson AF, MacLean JC, Fryer RJ. Rod catch trends for early-running MSW salmon in Scottish rivers (1952–1997): divergence among stock components. ICES J Mar Sci 2002;59:836–49.
Zimmermann AE, Lapointe M. Intergranular flow velocity through salmonid redds: sensitivity to fines infiltration from low intensity sediment transport events. River Res Appl 2005;21:865–81.